

# Transport Coefficients of Expanded Fluid Metals

H. von Tippelskirch

Institut für Physikalische Chemie und Elektrochemie,  
Universität Karlsruhe, Karlsruhe, Germany

Z. Naturforsch. **32 a**, 1146–1151 [1977]; received July 14, 1977)

The viscosities and the self-diffusion coefficients of expanded fluid mercury and caesium have been calculated as a function of pressure and temperature up to their critical points with the aid of a modified Enskog theory. The results are compared with the transport coefficients of other liquid metals and of non-polar and polar fluids applying the principle of corresponding states. The thermal conductivities of fluid metals along the full coexistence line are also discussed. A classification of the transport phenomena in fluids with various types of interaction forces — including expanded fluid metals — is given.

## 1. Introduction

Continuous transitions from metal to non-metal behaviour have been found in a number of fluid systems<sup>1</sup>. In pure expanded metals above their critical points, for example, the gradual variation of temperature or pressure can cause the electronic state and thus the nature of interaction forces to be changed. As well as the known behaviour of electrical properties, the “classical” transport coefficients, diffusion, viscosity and thermal conductivity are strongly affected by this transition.

However, even in normal simple fluids, the transport phenomena respond characteristically to an increase in density<sup>2</sup>. To study the effects specific for the metal-nonmetal transition, the normal density dependence should be accounted for in a proper way.

One possible method implies the application of the principle of corresponding states<sup>3</sup>: if the interaction potential has a similar form for different substances, reduced thermodynamic variables are universal functions of reduced temperature and pressure for this class of fluids. Different reduced charts for two given substances can be attributed to different interaction potentials. Variation of the interaction potential as a result of density expansion in a single fluid can be detected.

Other approaches utilize theoretical calculations of the transport coefficients as a function of pressure and temperature. Application of the Modified Enskog Theory<sup>4</sup> yields results which describe the transport coefficients in terms of an effective hard-sphere diameter.

In the following, the general features of transport phenomena in expanded fluid metals will be discussed with emphasis on the influence of the metal-nonmetal transition. Since at present the experimental data are concentrated on the saturation line, the comparison will be mostly limited to the coexistent phases.

## 1. Enskog Theory of Transport Phenomena in Fluids

In dilute monatomic gases, thermal energy, momentum and mass are propagated by translational transport. In compressed, dense gases, where the mean interatomic distance and the molecular diameters are of comparable size, collisional transfer comes into play as well, eventually dominating the thermal energy and momentum transport. For diffusion processes, however, translation is the only possible mechanism which becomes increasingly hindered during compression. The influence of density on the three types of transport, therefore, causes a change in their mutual relationships from the dilute-gas limit to the liquid-density limit. Whereas the proportionality of the self-diffusion coefficient, the viscosity and the thermal conductivity predicted by kinetic gas theory is very well verified in dilute gases, in liquids the Stokes-Einstein behaviour is observed. This demanding the self-diffusion coefficient to be proportional to the reciprocal of viscosity.

The Enskog theory provides a description of transport phenomena throughout the full compression range for fluids composed of small, non-polar and spherical molecules. In such fluids, energy and momentum transport processes are caused by the same type of molecular mechanism. In fluids with

Reprint requests to Dr. H. v. Tippelskirch, Institut für Physikalische Chemie und Elektrochemie, Universität Karlsruhe, Kaiserstr. 12, D-7500 Karlsruhe.



Dieses Werk wurde im Jahr 2013 vom Verlag Zeitschrift für Naturforschung in Zusammenarbeit mit der Max-Planck-Gesellschaft zur Förderung der Wissenschaften e.V. digitalisiert und unter folgender Lizenz veröffentlicht: Creative Commons Namensnennung-Keine Bearbeitung 3.0 Deutschland Lizenz.

Zum 01.01.2015 ist eine Anpassung der Lizenzbedingungen (Entfall der Creative Commons Lizenzbedingung „Keine Bearbeitung“) beabsichtigt, um eine Nachnutzung auch im Rahmen zukünftiger wissenschaftlicher Nutzungsformen zu ermöglichen.

This work has been digitalized and published in 2013 by Verlag Zeitschrift für Naturforschung in cooperation with the Max Planck Society for the Advancement of Science under a Creative Commons Attribution-NoDerivs 3.0 Germany License.

On 01.01.2015 it is planned to change the License Conditions (the removal of the Creative Commons License condition “no derivative works”). This is to allow reuse in the area of future scientific usage.

polar or large non-spherical molecules the internal degrees of freedom of the molecules do not contribute to the viscosity in the same manner as they do to thermal conduction. An approximation introduced by Eucken<sup>5</sup> could take account for this effect.

The Enskog equations of the transport coefficients in dense gases are<sup>3</sup>:

$$\text{self-diffusion } \varrho \cdot D_E = b/v \cdot (b/v \chi)^{-1} \cdot \varrho_0 \cdot D_0,$$

viscosity

$$\eta_E = b/v((b/v \chi)^{-1} + 0.800 + 0.761(b/v \chi)) \eta_0,$$

thermal conduction

$$\lambda_E = b/v((b/v \chi)^{-1} + 1.200 + 0.755(b/v \chi)) \lambda_0.$$

The Enskog dense gas coefficients are expressed as functions of the dilute gas limits, denoted by the subscript 0. The dilute-gas coefficients can be evaluated from the theory of Chapman-Enskog<sup>3</sup>. Here, the solutions for a gas, made up of molecules interacting under the hard-sphere potential, are given by:

$$\begin{aligned} \varrho_0 D_0 &= s_D 3/8 (\pi m k T)^{1/2} (\pi \sigma^2)^{-1}, \\ \eta_0 &= s_\eta 5/16 (\pi m k T)^{1/2} (\pi \sigma^2)^{-1}, \\ \lambda_0 &= s_\lambda 75/64 (\pi k^3 T m^{-1})^{1/2} (\pi \sigma^2)^{-1}. \end{aligned}$$

$\sigma$  is the hard-sphere diameter,

$b = 2\pi/3 \sigma^3 m^{-1}$  is the second virial coefficient,

$b/v \chi = pV/RT - 1$ , which is the equation of state of a hard-sphere fluid.  $V$  is the molar volume,  $m$  is the molecular mass, and  $v$  the volume per unit mass. The Sonine expansion polynomial correction terms are dimensionless numbers denoted by

$$s_D = 1.1333, \quad s_\eta = 1.0160, \quad s_\lambda = 1.0246.$$

In Enskog's derivation the directional and velocity distribution functions of colliding particles are taken to be completely random. Alder, Gass and Wainwright<sup>6</sup> investigated the assumption of molecular chaos in their molecular dynamics computer simulations. They evaluated a more realistic decay of the van Hove autocorrelation-function by hard-sphere collisions. The effect of correlated molecular motion on the transport coefficients is considered by multiplying the Enskog equations with correction functions

$$F_D(b/v) = D/D_E, \quad F_\eta(b/v) = \eta/\eta_E, \quad F_\lambda(b/v) = \lambda/\lambda_E.$$

Their numerical values are tabulated as functions of the relative density in <sup>7</sup>.

The equations finally obtained are:

$$\varrho \cdot D = b/v(b/v \chi)^{-1} \cdot \varrho_0 \cdot D_0 \cdot F_D(b/v), \quad (1)$$

$$\eta = b/v((b/v \chi)^{-1} + 0.800 + 0.761(b/v \chi)) \cdot \eta_0 \cdot F_\eta(b/v),$$

$$\lambda = b/v((b/v \chi)^{-1} + 1.200 + 0.755(b/v \chi)) \cdot \lambda_0 \cdot F_\lambda(b/v),$$

$$b = 2\pi/3 \cdot \sigma^3 \cdot m^{-1}.$$

The unique parameter in the theory, the molecular diameter  $\sigma$  can be determined by analysis of experimental PVT-data. Thus the theory allows the prediction of transport coefficients — that is, non-equilibrium phenomena — from equilibrium properties.

## 2. Application of the Enskog Theory to Fluid Metals

A model description of a weakly interacting binary mixture has been successful in interpreting thermodynamic and transport phenomena in metals. The mixture is thought to be made of a delocalized Fermi electron gas embedded in an ion matrix. In fluid metals the ions are equally free to move and are able to contribute to transport processes by an extent depending on the conditions. In the metallic liquid range, viscosity is mainly due to the motions of the ions, whereas thermal energy is mostly conducted by motions of the electrons. The ions contribute to thermal conduction only by a few percent. By definition, self-diffusion is due to the ions' motions.

The situation is completely altered beyond the metal-nonmetal transition. By a sufficiently large expansion of the liquid metal the nature of interaction forces is changed. The electrons become localized on the ions forming neutral particles in thermal equilibrium with some electronically excited or ionized species. Since the metal-nonmetal transition alters the interaction forces, the effective cross-sections are also changed. This has been approximated in the current investigation by splitting the PVT-surface into two regions, the metallic liquid and the nonmetallic vapour range, where different effective diameters are assumed to apply. Each diameter has been taken to be a function of temperature, but not of volume. The neglect of the volume effect seems tolerable considering the viscosity of liquid mercury near room temperature<sup>8</sup>,

where isothermal experimental data are available<sup>9</sup>, though a volume dependence of a more realistic pseudopotential in liquid metals is well established by theory<sup>10</sup>.

### 3. Evaluation of the Effective Diameters

The temperature dependence of the effective diameter could be approximated with sufficient accuracy by the function

$$\sigma = \sigma_m (T_m/T)^x.$$

The melting point was chosen for reference and denoted by the subscript <sub>m</sub>. The liquid metal value  $\sigma_m$  was calculated from the packing fraction at the melting point, which was taken  $(b/v)_m = 1.900$  to be constant for the metals concerned. This value is slightly higher than that derived from neutron scattering experiments. The exponent  $x$ , which accounts for the somewhat soft repulsive energy, has been fitted to high temperature PVT-data of mercury metal and assumed to be the same for all metals. The fitting procedure proposed by Alder et al.<sup>7</sup> has been adopted which makes use of the van der Waals' fluid concept.

The appropriate parameters of the nonmetal vapour range were fitted to the low density, viscosity data<sup>11</sup>. The parameters are listed in Table 1.

Table 1. Hard-sphere parameters of metals in the liquid and vapour ranges.

	liquid metal range		vapour range	
	$\sigma_m \times 10^{10} \text{ (m)}$	$x$	$\sigma_m \times 10^{10} \text{ (m)}$	$x$
Hg	2.81	0.091	4.93	0.285
Cs	4.79	0.091	9.25	0.285
Na	3.34	0.091		
Ga	2.56	0.091		
Pb	3.08	0.091		

### 4. The Viscosity of Liquid Metals

The model described in the previous sections was applied to calculate the viscosity of liquid metals along the saturation line. As a test of consistency, experimental data were compared with the predicted values over a wide range of temperatures. The results are shown in Fig. 1, where the viscosity of several liquid metals is plotted as a function of temperature. The experimental data have been obtained for lead by Cakici<sup>12</sup>, for mercury by v. Tip-

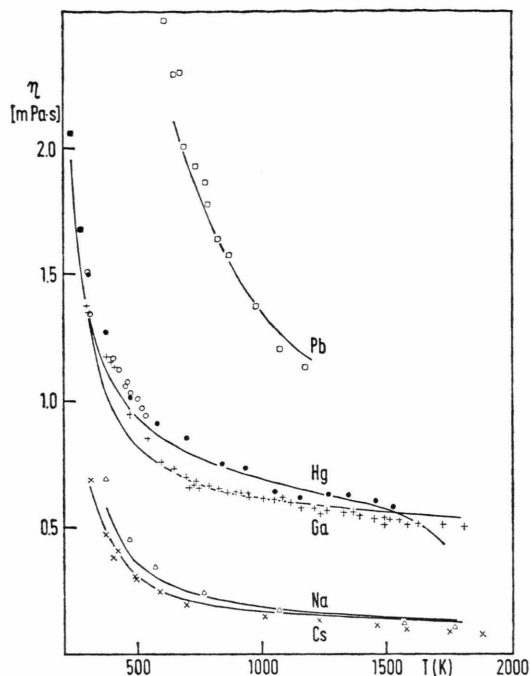


Fig. 1. Viscosity of liquid metals. The line were calculated using Enskog's theory. Pb: □ Cakici<sup>12</sup>; Hg: ■ Suhrmann<sup>27</sup>; ○ Grouvel<sup>13</sup>; ● v. Tippelskirch<sup>11</sup>; Ga: + v. Tippelskirch<sup>14</sup>; Na: △ Achener<sup>15</sup>; Cs: × Tsai<sup>16</sup>.

pelskirch et al.<sup>11</sup> and Grouvel et al.<sup>13</sup>, for gallium by v. Tippelskirch<sup>14</sup>, for sodium by Achener<sup>15</sup> and for caesium by Tsai et al.<sup>16</sup>.

It is clearly seen that the general trend of the data points is well reproduced by the calculated lines, though the deviations are still greater than the limits of experimental errors. Nevertheless, the evidently simple behaviour of liquid metals with respect to viscosity is described by such a one-parameter model, whose physical meaning seems to be more justified than Eyring's approach<sup>17</sup>. Thus the extrapolation to even higher temperatures up to the critical point seems permissible.

### 5. Viscosity of Caesium in the Critical Range

In Fig. 2 the viscosity of caesium is shown as a function of temperature along the full coexistence curve. The experimental data are taken from Tsai et al.<sup>16</sup>, Lee et al.<sup>18</sup> and v. Tippelskirch<sup>14</sup>. The upper line, as with Fig. 1, shows the viscosity of the liquid calculated with the metal parameters of Table 1. The dotted extension of this line represents the extrapolation beyond the critical point at

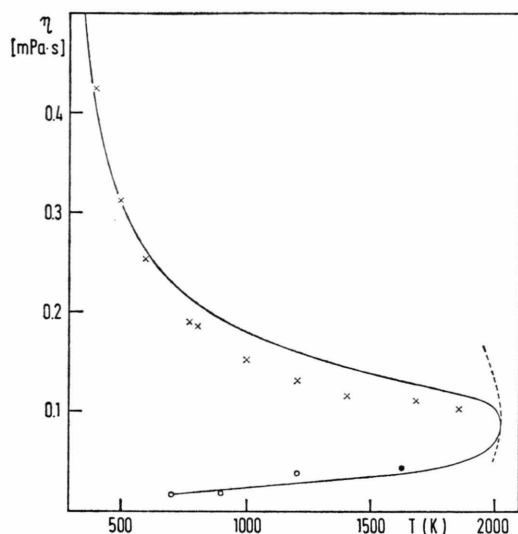


Fig. 2. Viscosity of caesium along the saturation line. — calc. using Enskog's theory.  $\times$  Tsai<sup>16</sup>;  $\bullet$  v. Tippelskirch<sup>14</sup>;  $\circ$  Lee<sup>18</sup>.

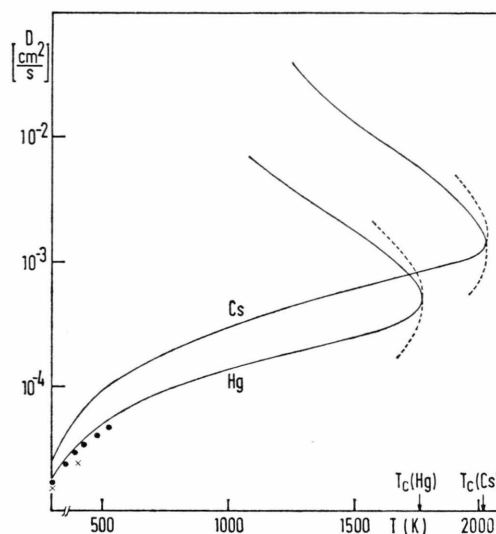


Fig. 3. Self-diffusion coefficients of mercury and caesium along the saturation line; — calc. using Enskog's theory.  $\times$  Nachtrieb<sup>19</sup>;  $\bullet$  Broome<sup>20</sup>.

volumes larger than the critical volume. The lower, full line shows the saturated vapour viscosity utilizing the vapour parameters. The dashed extension is the hypothetical extrapolation to volumes smaller than the critical. Although the situation in reality is more complicated than that represented by the model calculation, which neglects dimerization and electronic excitation in the high-temperature gas, the present experimental results are too scarce to justify a further refinement of the theory.

From the intersection of both metal and non-metal lines a critical viscosity of  $\eta_c = 0.09$  (mPa · s) is derived. From the experiment a critical viscosity of  $\eta_c = 0.074$  (mPa · s) seems reasonable. Tsai et al.<sup>16</sup> quoted a value of  $\eta_c = 0.057$  (mPa · s), which is possibly somewhat too small.

## 6. Diffusion Coefficients of Mercury and Caesium

Since the experimental determination of self-diffusion is extremely difficult, especially in the high temperature region, predictions based on viscosity data would be valuable. In liquids, the Stokes-Einstein relationship is frequently used, but ceases to be valid upon expansion. The Enskog theory, however, yields a relationship valid throughout the interesting density range. Utilizing the parameters of Table 1 and Eq. 1, the self-diffusion coefficients of mercury and caesium have been calculated along

the coexistence line. They are plotted in Fig. 3 on a logarithmic scale as a function of temperature. Experimental data, existing at present in the liquid range near the melting point, are also recorded. These have been taken from Nachtrieb<sup>19</sup> and Broome<sup>20</sup>. Diffusion is small in the liquid as expected and, though it becomes larger with increasing temperature, volume expansion increases diffusion to an even greater extent. The highest values are therefore found in the vapour region. The curves, which have been calculated with the metal parameters, intersect the curves derived from the vapour diameter in the neighbourhood of the critical point. The dotted lines represent the mutual hypothetical extrapolation beyond the critical volumes.

## 7. The Reduced Viscosity Diagram

Variations of temperature and pressure influence the viscosity of various fluids in a similar way. The pressure coefficient is always positive, whereas the temperature coefficient, which is always negative at high density, changes sign upon isothermal expansion to large volumes.

In comparing thermodynamic and transport properties of different substances, reduced quantities, rather than the variables themselves, have been successfully introduced. They are given by the ratio of the value at a certain point to some reference value. Often the critical point is chosen for reference.

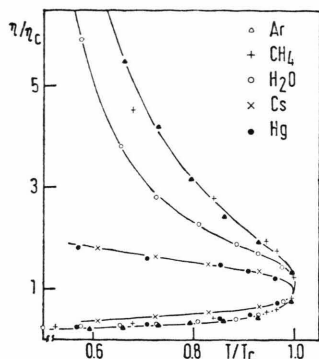


Fig. 4. Viscosity of metallic, polar and non-polar fluids along the saturation line, reduced units.

Such reduced functions are universal in a class of substances with similar interaction forces. This statement is contained in the principle of corresponding states.

On the other hand conclusions for a classification of interaction forces may be drawn from individual behaviour in the reduced diagrams. In Fig. 4 the viscosities of various fluids under saturation conditions are shown as a function of temperature in reduced units. The experimental points have been taken from Vasserman<sup>21</sup> for argon, Zagoruchenko<sup>22</sup> for methane and Brown et al.<sup>23</sup> for water. The lines — orthobars — are fitted to the experimental results. The density along the orthobars varies with temperature from low, dilute-gas values at the lower left-hand corner of the diagram to liquid densities at the upper end of the curves. At a given reduced temperature, the relative viscosities of the non-polar fluids argon and methane on the liquid branches are greater than that of the strongly polar fluid water. This in turn is greater than the relative viscosities of the liquid metals caesium and mercury. A similar sequence holds for the fluidity in the expanded vapour region, so that the difference between vapour and liquid viscosity decreases from argon to caesium by about a factor of three.

### 8. The Reduced Diffusion Coefficient Diagram

For the same reasons as for the viscosity, the calculated and experimental self-diffusion coefficients for various substances were compared in a reduced program. They are shown in Fig. 5, where the diffusion coefficients are plotted in a reduced logarithmic scale as a function of reduced temperature. The experimental values for water and benzene from Hausser<sup>24</sup> have been measured by the

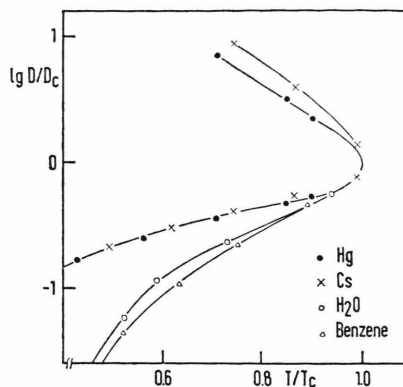


Fig. 5. Self-diffusion coefficients of metallic, polar and non-polar fluids, reduced units in a semi-logarithmic scale.

spin-echo method. The curves for mercury and caesium have been calculated from Figure 3.

At a given reduced temperature, the relative diffusion is more rapid in liquid metals than in water and benzene. The sharp increase with temperature is common for all four substances. The vapour curves have not yet been experimentally investigated.

### 9. The Reduced Thermal Conductivity Diagram

In Fig. 6 the thermal conductivity is shown for several fluids, mercury, caesium, water and xenon.

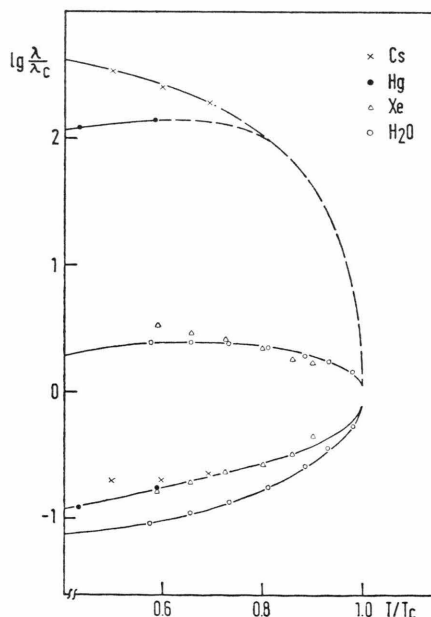


Fig. 6. Thermal conductivity of metallic, polar and non-polar fluids, reduced units, semilogarithmic scale.

The experimental points were taken from Vargaftik<sup>25</sup>. Again a reduced, logarithmic scale was used in plotting thermal conductivity as a function of reduced temperature. The reference values (i.e. the conductivity at the critical points) were obtained by fitting the vapour thermal conductivity of the four substances at a reduced temperature of 0.7. Thus the singularity in the critical region has been excluded from the evaluation of the reference values.

The non-polar and polar fluids, xenon and water, show the familiar tongue-shaped saturation line, where the lower branch yields the vapour thermal conductivity line and the upper branch represents the saturated liquid curve. This part exhibits a maximum in thermal conductivity at a temperature, where the increase in heat capacity is balanced by the volume expansion effect.

The reduced thermal conductivity of caesium and mercury along the saturated-liquid line is about a hundred times larger than in water. Thus

the electronic contribution to the transport of heat may be no longer neglected. The electronic thermal conductivity can be calculated, using the Wiedemann-Franz law, from the electrical conductivity and the theoretical Lorenz ratio predicted by Sommerfeld. Measurements of the Lorenz ratio in liquid tin carried out by Güntherodt et al.<sup>26</sup> yielded excellent agreement with the theoretical value, in fact within 1%. This allows the conclusion that the electronic contribution is indeed the dominating process. The ionic contribution can be calculated with the Enskog theory, as it has been for viscosity and diffusion. The results of the calculation yielded small enough values to neglect the ionic contribution to thermal conduction on the present level of accuracy in the metallic range.

The author expresses his appreciation to Prof. Dr. E. U. Franck for helpful discussion and advice, and to Mr. S. Luck, Guildford for assistance with the English language.

- <sup>1</sup> F. Hensel, Ber. Bunsenges. Physikal. Chem. **80**, 786 [1976].
- <sup>2</sup> E. U. Franck and W. Jost, Z. Elektrochem. **62**, 1054 [1958].
- <sup>3</sup> J. O. Hirschfelder, C. F. Curtiss, and R. B. Bird, Molecular Theory of Gases and Liquids, 2nd ed. J. Wiley and Sons, New York 1965.
- <sup>4</sup> H. J. M. Hanley, R. D. McCarty, and E. G. D. Cohen, Physica **60**, 322 [1972].
- <sup>5</sup> A. Eucken, Physik. Z. **14**, 324 [1913].
- <sup>6</sup> B. J. Alder, D. M. Gass, and T. E. Wainwright, J. Chem. Phys. **53**, 3813 [1970].
- <sup>7</sup> J. H. Dymond and B. J. Alder, J. Chem. Phys. **43**, 2061 [1966].
- <sup>8</sup> H. v. Tippelskirch, Thesis, Karlsruhe 1973.
- <sup>9</sup> P. W. Bridgman, The Physics of High Pressure. Bell, London, repr. 1958, p. 346.
- <sup>10</sup> V. Heine, Solid State Phys. **24**, 1 [1970].
- <sup>11</sup> H. v. Tippelskirch, E. U. Franck, F. Hensel, and J. Kestin, Ber. Bunsenges. Physikal. Chem. **79**, 889 [1975].
- <sup>12</sup> T. Cakici, Thesis, TU Berlin 1976, FB Werkstoffwissenschaften.
- <sup>13</sup> J. M. Grouvel, J. Kestin, H. E. Khalifa, E. U. Franck, and F. Hensel, Ber. Bunsenges. Physikal. Chem. **81**, 338 [1977].
- <sup>14</sup> H. v. Tippelskirch, Ber. Bunsenges. Physikal. Chem. **80**, 726 [1976].
- <sup>15</sup> P. Y. Achener and M. R. Boyer, AGN-8192, Vol. 3.
- <sup>16</sup> H. C. Tsai and D. R. Olander, High Temp. Sci. **6**, 142 [1974].
- <sup>17</sup> B. J. Alder and T. Einwohner, J. Chem. Phys. **43**, 3399 [1965].
- <sup>18</sup> C. S. Lee, D. I. Lee, and C. F. Bonilla, Nucl. Eng. Des. **10**, 83 [1969].
- <sup>19</sup> N. H. Nachtrieb and J. Petit, J. Chem. Phys. **24**, 746 [1956].
- <sup>20</sup> E. F. Broome and H. A. Walls, TMS-AIME **242**, 2177 [1968].
- <sup>21</sup> A. A. Vasserman and V. A. Rabinovich, Thermophysical properties of liquid air and its components, Moscow 1968.
- <sup>22</sup> V. A. Zagoruchenko and A. M. Zhuravlev, Thermophysical properties of methane, Standard Press, 1969.
- <sup>23</sup> O. L. L. Brown, H. E. Cary, G. S. Skinner, and E. J. Wright, J. Phys. Chem. **61**, 103 [1957].
- <sup>24</sup> R. Häusser, G. Maier, and F. Noak, Z. Naturforsch. **21a**, 1410 [1966].
- <sup>25</sup> N. B. Vargaftik, Tables on the Thermophysical properties of liquids and gases, engl. transl. J. Wiley and Sons, New York 1975.
- <sup>26</sup> W. Haller, H. J. Güntherodt, and G. Busch, in: R. Evans, D. A. Greenwood, ed., Liquid Metals 1976, Conf. Ser. Nr. 30, p. 207–211. The Institute of Physics Bristol and London.
- <sup>27</sup> R. Suhrmann and E. O. Winter, Z. Naturforsch. **10a**, 985 [1955].